Electronic supplementary information

Adsorption and Intercalation of Organic Pollutants and Heavy Metal Ions into MgAl-LDHs Nanosheets with Super High Capacity

Jian Li, Hongzhi Cui, Xiaojie Song, Guosong Zhang, Xinzhen Wang, Qiang Song, Na Wei, Jian Tian**

School of Materials Science and Engineering, Shandong University of Science and Technology, Qingdao 266590, China. Email: cuihongzhi1965@163.com; jiantian@sdust.edu.cn

1. Standard curve of MO, Cr(VI) and Ni(II) solution

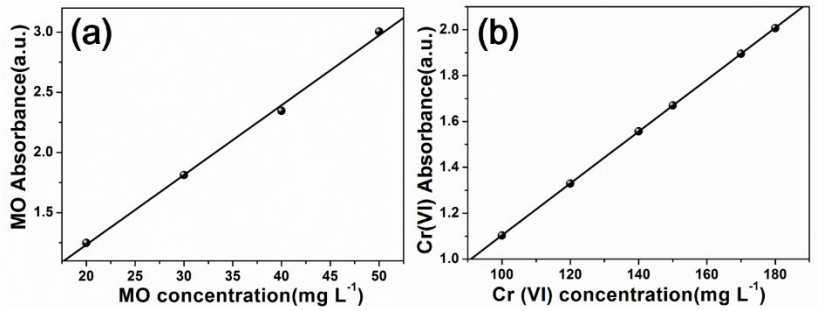

Fig. S1. The relative absorbance of aqueous (a) MO and (b) Cr(VI) solution as function of initial concentration. (R_a^2=0.999, R_b^2=0.999).

By testing the absorbance of (a) MO and (b) Cr(VI) aqueous solution with different concentrations, a linear relationship between the concentration and the absorbance was established and is shown in Fig. S1.

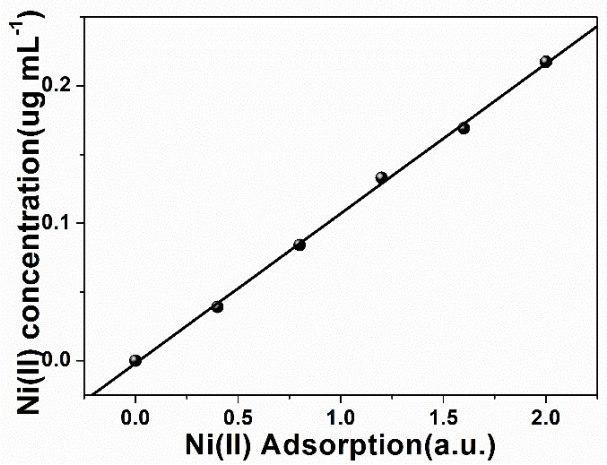

Fig. S2. The relative absorbance of Ni(II)-dimethylglyoxime complex after adsorption as function of initial concentration. (R^2=0.999).

Fig. S2 are shown the Ni(II)-dimethylglyoxime linear relationship (R^2 = 0.999) between the initial concentration and solution absorbance.

2. Particle size distribution of MgAl-LDHs nanosheets and microsheets.

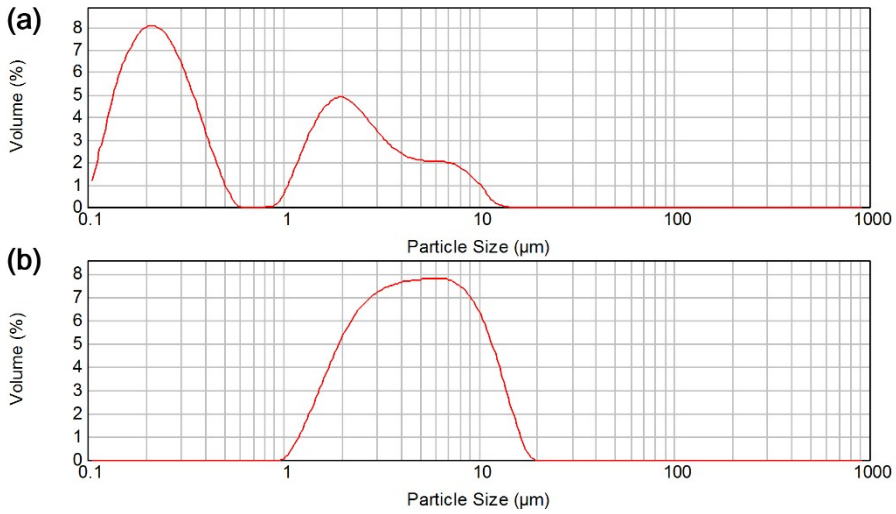

Fig. S3. Particle size distribution of MgAl-LDHs (a) nanosheets and (b) microsheets.

Particle size distribution of MgAl-LDHs nanosheets and microsheets are shown in Fig S3. The particle sizes of MgAl-LDHs nanosheets (Fig. S3(a)) are about 200 ± 100 nm and 2 ±1 μm. The latter values may be due to the agglomeration of nanosheets. Besides, the particle sizes of MgAl-LDHs nanosheets is smaller than those of microsheets (5 ± 1 μm)(Fig. S3(b)).

3. Comparisons of adsorption performance of MgAl-LDHs nanosheets and microsheets

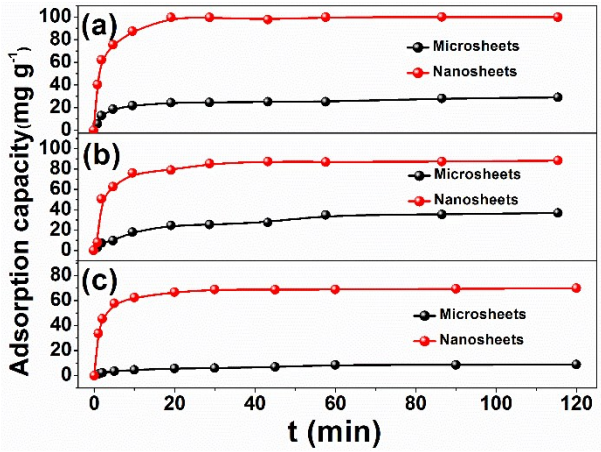

Fig. S4. Adsorption performance of (a) MO, (b) Cr(VI) anions and (c) Ni(II) cations for MgAl-LDHs nanosheets and microsheets.

The adsorption performance of MO, Cr(VI) anions, and Ni(II) cations for MgAl-LDHs nanosheets and microsheets, as shown in Fig. S4. The results give clear evidence that MgAl-LDHs have have excellent adsorption capacity for organic pollutants and heavy metal ions. The MgAl-LDHs nanosheets exhibit much higher adsorption and the adsorption at equilibrium amount can reach 99.9, 88.3 and 69.9 $mg \cdot g^{-1}$ for the adsorption of MO, Cr(VI) anions and Ni(II) cations, respectively, values that are much higher than those of the microsheets (29.1, 37.0 and 8.9 $mg \cdot g^{-1}$). Furthermore, the adsorption rate of MO, Cr(VI) anions, Ni(II) cations for MgAl-LDHs nanosheets was still superior to microsheets. The excellent adsorption capacity of organic pollutants and heavy metal ions can be attributed to the larger specific surface area and the smaller in width of the MgAl-LDHs nanosheets.

4. The adsorption kinetics and the adsorption isotherms of Cr(VI) and Ni(II).

The adsorption of Cr(VI) anion and Ni(II) cation for the MgAl-LDHs nanosheets are consistent with both the pseudofirst-order and pseudosecond-order equations (Fig. S5), and the correlation coefficient (listed in Table S1) for the pseudosecond-order model ($R^2 = 1.000$) is appreciably larger that of the pseudofirst-order model ($R^2 < 0.985$). As a general observation, the best-fit pseudosecond-order parameters (q_e) is little different with equilibrium adsorption capacity.

Table S1 Parameters of pseudofirst-order and pseudosecond-order for adsorption of Ni(II) and Cr(VI) for LDHs nanosheets.

	Pseudofirst-order			Pseudosecond-order		
	$\log(q_e - q_t) = \log(q_e) - k_1/2.303t$			$t/q_t = 1/(k_2 q_e^2) + t/q_e$		
	k_1 min^{-1}	q_e $mg \cdot g^{-1}$	R^2	k_2 $mg^{-1} \cdot g \cdot min^{-1}$	q_e $mg \cdot g^{-1}$	R^2
Cr(IV)	0.040	4.253	0.913	0.021	89.286	1.000
Ni(II)	0.032	2.238	0.984	0.013	70.423	1.000

where q_t ($mg \cdot g^{-1}$) is the adsorption capacity at time t (min); q_e ($mg \cdot g^{-1}$) is the equilibrium adsorption capacity; and k_1 and k_2 are related to pseudo first-order and pseudo second-order apparent adsorption rate constants.

The outstanding adsorption capacity is also reflected by the linear fitting of the Langmuir and Freundlich isotherms (Fig. S6), the results obtained from the isotherms are calculated in Table S2. According to the values of R^2 of the two isotherms, as described herein, the Langmuir Freundlich equation is higher than the Freundlich

equation, which indicates that the Langmuir isotherms provide a better fit for the experimental data.

Table S2 Parameters of Freundlich and Langmuir models for adsorption of Cr(VI) anions and Ni(II) cations for LDHs nanosheets.

	Langmuir			Freundlich		
	$c_e/q_e = 1/(bq_{max}) + c_e/q_{max}$			$\log q_e = \log k_3 + 1/n \log c_e$		
	q_{max} $mg \cdot g^{-1}$	b $L \cdot mg^{-1}$	R^2	K_1 $mg \cdot g^{-1}(L \cdot mg^{-1})^{1/n}$	n	R^2
Cr(IV)	63.8	38.808	0.999	51.800	11.062	0.753
Ni(II)	92.3	1.874	0.999	64.096	8.440	0.796

where c_e is equilibrium adsorbate concentration ($mg \cdot L^{-1}$); q_e is the equilibrium adsorption capacity ($mg \cdot g^{-1}$); q_{max} ($mg \cdot g^{-1}$) and b ($mg \cdot L^{-1}$) correspond to the maximum adsorption capacity and the adsorption energy, respectively; and k_3 and n are related to Freundlich isotherm constants.

5. The cyclic utilization of the MgAl-LDHs nanosheets for adsorption of Cr(VI)

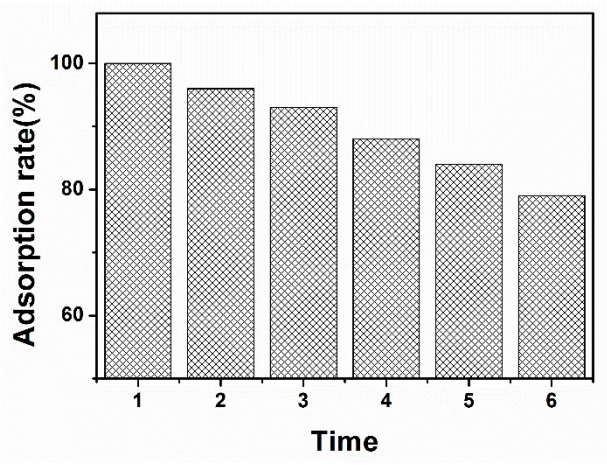

Fig. S5. Cyclic utilization of the MgAl-LDHs nanosheets for the adsorption of Cr (VI).

The cyclic utilization of the adsorbent for adsorption of Cr(VI) was carried out after it was regenerated by washing three times with deionized water (shown in Fig. S5). It is found that the MgAl-LDHs nanosheets exhibits a very stable performance on adsorption of Cr(VI). The adsorption rate is only reduced by approximately 20% after five cycles.